Available online at www.sciencedirect.com
ScienceDirect
Journal of Power Sources 172 (2007) 845–852
JOURNAL OF POWER SOURCES
www.elsevier.com/locate/jpowsour

Performance improvement of diesel autothermal reformer by applying ultrasonic injector for effective fuel delivery

Inyong Kang [a], Joongmyeon Bae [a,*], Sangho Yoon [a], Youngsung Yoo [b]

[a] *Department of Mechanical Engineering, Korea Advanced Institute of Science and Technology (KAIST), Daejeon, South Korea*
[b] *Strategic Technology Laboratory, Korea Electric Power Research Institute (KEPRI), Daejeon, South Korea*

Received 7 March 2007; accepted 10 May 2007
Available online 18 May 2007

Abstract

Technology for the reforming of heavy hydrocarbons, such as diesel, to supply hydrogen for fuel cell applications is very attractive and challenging due to its delicate control requirements. The slow reforming kinetics of aromatics contained in diesel, sulfur poisoning, and severe carbon deposition make it difficult to obtain long-term performance with high reforming efficiency. In addition, diesel has a critical mixing problem due to its high boiling point, which results in a fluctuation of reforming efficiency. An ultrasonic injector (UI) have been devised for effective diesel delivery. The UI can atomize diesel into droplets (~40 μm) by using a piezoelectric transducer and consumes much less power than a heating-type vapourizer. In addition, reforming efficiencies increase by as much as 20% compared with a non-UI reformer under the same operation conditions. Therefore, it appears that effective fuel delivery is linked to the reforming kinetics on the catalyst surface. A 100-W_e, self-sustaining, diesel autothermal reformer using the UI is designed. In addition, the deactivation process of the catalyst, by carbon deposition, is investigated in detail.

Keywords: Hydrogen; Fuel cell; Reforming efficiency; Diesel; Ultrasonic injector; Autothermal reforming

1. Introduction

Fuel reforming is a practical method to produce hydrogen for fuel cell applications. Numerous efforts to reform fossil fuels such as natural gas, LPG, gasoline, and diesel have been tried. Diesel reforming, as a fuel supply for fuel cells, has been considered to be the most challenging technology. It has a high potential for application in a variety of industrial fields such as automobiles (propulsive or auxiliary power generation), distributed power generation, and power generation for military purposes, etc. In addition, there is a report of using an on-board diesel reformer for internal combustion engines in low-emission vehicles [1]. In spite of these possible applications, diesel reformers are still not ready for commercialization. Most of all, it is difficult to inhibit carbon deposition [1–8]. Carbon deposition occurs easily on the catalyst surface, even though operation is conducted in the thermodynamically carbon-free zone [9]. Kinetic factors, such as the relative reaction rates of the various components in the fuel and the nature of the catalyst, may influence carbon deposition [8]. Sulfur poisoning has also been reported [4,10–13] to prevent the development of a diesel reformer with stable long-term performance.

In addition, technical issues such as effective diesel delivery should be considered. It is difficult to vapourize diesel due to its wide range of high boiling points. Its high viscosity also leads to flow pulsation when using a liquid pump. In diesel-related fields, such as the internal combustion engine, diesel is usually delivered into the combustion chamber by means of a high pressure injector. Diesel injected by the high pressure injector is atomized into micron-sized droplets in the form of a spray. This helps to increase each of the following: the fuel-free surface area, evaporation, mixing with air, and combustion rates. Generation of the mixture constitutes a key factor in the quality of the chemical reaction [14]. It is slightly difficult, however, to adapt a high-pressure injector to diesel reforming because injecting diesel at high pressure can cause poor mixing of the fuel and oxidants (air and/or steam) as they come into contact with the catalyst surface. This can result in excessively high temperatures that can damage or destroy the catalyst [8].

* Corresponding author. Tel.: +82 42 869 3045; fax: +82 42 869 8207.
E-mail address: jmbae@kaist.ac.kr (J. Bae).

0378-7753/$ – see front matter © 2007 Elsevier B.V. All rights reserved.
doi:10.1016/j.jpowsour.2007.05.033

This study reports the development of an ultrasonic injector (UI, U.S. patent pending: 11//549,359) for effective diesel delivery. The UI uses mechanical force to atomize the diesel by a piezoelectric transducer. On the basis of previous research [9,15–18], a 100-W_e self-sustaining diesel UI reformer has been designed.

2. Experimental

Two types of reactors were prepared for studying diesel reforming. One is a micro-reactor controlled by an electrical furnace to test the effect of the UI on reforming performance. The other is a 100-W_e-class engineering reactor insulated with a ceramic material on the reactor wall instead of an electrical furnace (a so-called self-sustaining reformer). To obtain high efficiency, autothermal reforming (ATR) technology is used to process diesel. This is a combination of steam reforming (SR) and partial oxidation (POX) [15]. Therefore, three pipe lines were prepared for the delivery of the fuel, water, and air. In addition, a nitrogen line was also installed to carry the vapourized water (steam). The fuel and water were delivered using an HPLC pump (MOLEH Co. Ltd.). The fuel was atomized by the UI at the top of the reactor and ultra pure water (>15 MΩ) was vapourized by an external heat exchanger. A picture of the injector and specifications of the UI are shown in Fig. 1 and Table 1, respectively. The flowrates of air and nitrogen were controlled individually by mass flow controllers (MKS). The product gases were analyzed by a GC–MS (TCD and FID installed, Agilent 6890N) after moisture removal. A TCD using argon as the carrier gas was used to analyze the relative amounts of H_2, CO, CO_2, O_2 and N_2 and a FID using helium (He) as the carrier gas was used to analyze the relative amounts of CH_4, C_2H_2, C_2H_4, C_2H_6, C_3H_6, C_3H_8, *iso*-C_4H_{10}, normal-C_4H_{10}, normal-C_5H_{12}, C_6H_{12} (cyclo-hexane), C_6H_6 (benzene), and *iso*-C_8H_{18}.

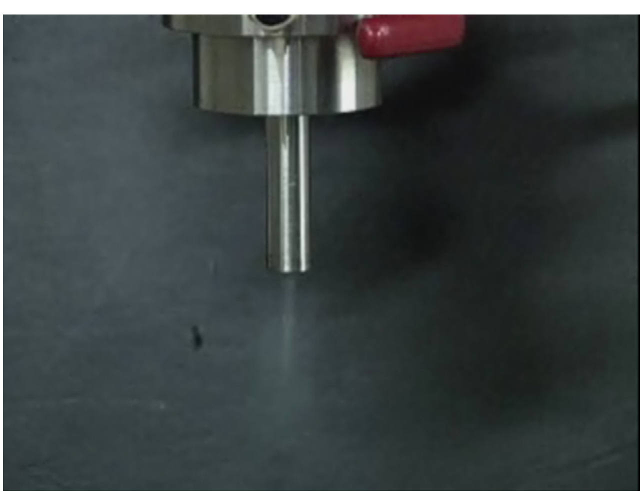

Fig. 1. Diesel injection through injector nozzle.

Table 1
Specifications of ultrasonic injector

Range of frequency	20–120 kHz
Power consumption (maximum)	22 W intermittent 15 W continuous
Droplet size	Average 40 μm

A catalyst of Pt on Gd-doped CeO_2 (CGO-Pt) was used to reform the diesel. A fine powder of the catalyst was prepared by the combustion spray method. The catalyst was pressed into pellets that were then crushed into granules of regular size (∼500 μm). The packed-bed reactors were made from stainless-steel (STS) tubes. A k-type thermocouple was installed at the top and at the bottom of the catalyst bed to monitor the reaction temperatures. The self-sustaining reactor employed catalyst granules with an average size of 855 μm. In addition, eight thermocouples were used to monitor temperatures at multiple positions inside the reactor.

Synthetic diesel (mixture of $C_{12}H_{26}$ and $C_{11}H_{10}$) and commercial diesel (GS-Caltex, Korea) were prepared for use as fuels in the autothermal reforming experiments. Previous studies have shown that the reforming performance of the synthetic diesel is in good agreement with commercial diesel [16]. Using synthetic diesel makes it easier to calculate the basic stoichiometries, such as O_2/C and H_2O/C, and the fuel conversion. After the experimental conditions were determined from synthetic diesel reforming, commercial diesel reforming was sequentially performed.

3. Results and discussion

A micro-reactor controlled by an electrical furnace was installed to investigate the effect of the UI on reforming performance. The experimental set-up is shown in Fig. 2. The total length and outer diameter of the reactor in the furnace are 50 cm and 1.27 cm, respectively. The GHSV (gas hourly space velocity at 25 °C, 1 atm) is 5000 h^{-1}.

Severe fluctuations of the inner temperatures and product concentrations in diesel autothermal reforming have been observed previously [15]. These may be caused by poor mixing of the fuel and oxidants (air and/or steam). The experimental set-up was modified to vapourize diesel efficiently at the reactor entrance (not described here) in order to minimize the mixing problem. Slightly improved concentration and temperature fluctuations (Fig. 3) were obtained compared with the previous performance [15].

Although slight improvements have been obtained, the issue with the fuel delivery essentially has not been resolved. When droplets of diesel of millimeter size were introduced into the reactor, due to an unforeseen reason, there was a very high probability of carbon formation as well as an unstable reforming reaction. This caused the performance of the reformer to decrease rapidly. The diesel requires vapourization or atomization, in order to solve the problem related with the fuel delivery issue. The former is not recommended due to large energy consumption, as well as increased system complexity. The latter is more favourable. A high-pressure nozzle injection was a representative-atomizing technique, but diesel injected at high speeds may come into contact with the catalyst surface or the reactor wall without mixing with the oxidants. In addition, a high-pressure gen-

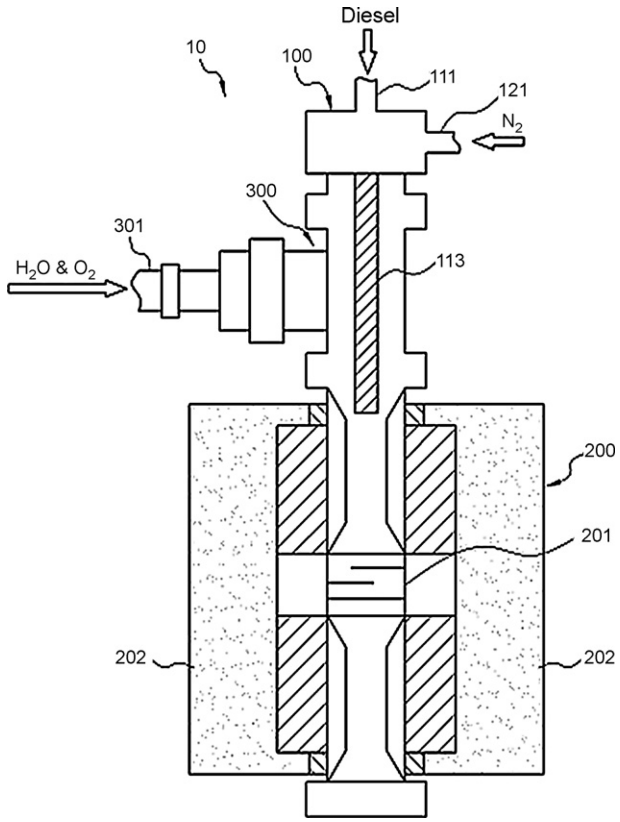

Fig. 2. Experimental set-up using ultrasonic device (100–113: ultrasonic device, 113: ultrasonic nozzle, 200: electrical furnace, 201: catalyst bed).

erator for the high-pressure injection increases the bulk-size of the reformer as well as the parasitic power consumption.

To solve the fuel delivery issue, we have devised an ultrasonic injector using a material with piezoelectricity. The diesel flowing through the ultrasonic nozzle is vibrated by the piezoelectric transducer at a high frequency (~60 kHz). Then, the bulk diesel is atomized into droplets of ~40 μm. The size distribution of the droplets was well-centralized around the average droplet size. The product compositions obtained from diesel reforming using the UI are given in Fig. 4. Although data fluctuations still exist, the reforming performance is surprisingly enhanced.

A comparison between the product distributions obtained from synthetic diesel reforming when the ultrasonic device was or was not being used is presented in Fig. 5. The solid line with symbols and the dotted line with symbols represent the relative amounts (mol% in H_2O and N_2-free basis) from the UI reformer and the non-UI reformer, respectively. The amounts of H_2 and CO produced were much greater with the UI reformer than with the non-UI reformer. Methane almost disappears at temperatures greater than 850 °C with the UI reformer. The lighter hydrocarbons are negligible at much less than 1 mol%. Almost 100% fuel conversion can be achieved at 800 °C, as seen in Fig. 6. The fuel conversion with the UI-reformer is 20% greater than that with the non-UI reformer under the same conditions (Fig. 7).

With respect to the reforming efficiency (RE), the results are very remarkable. The REs using $C_{16}H_{34}$ (hexadecane) as a surrogate fuel (left bar) and as a synthetic diesel (middle bar) in the non-UI reformer are 83% and 67%, respectively. The lower RE of synthetic diesel is due to the addition of aromatic compounds. Aromatic compounds cause the reforming kinetics to slow down, which has been well-reported [1,8,12]. On the other

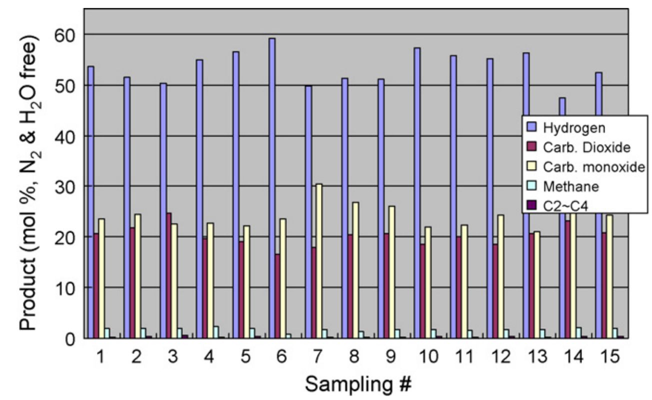

Fig. 4. Product compositions according to time (synthetic diesel, $H_2O/C = 1.25$, $O_2/C = 0.5$, 5000 h^{-1},CGO-Pt, furnace temperature = 800 °C, average fuel conversion = ~100%).

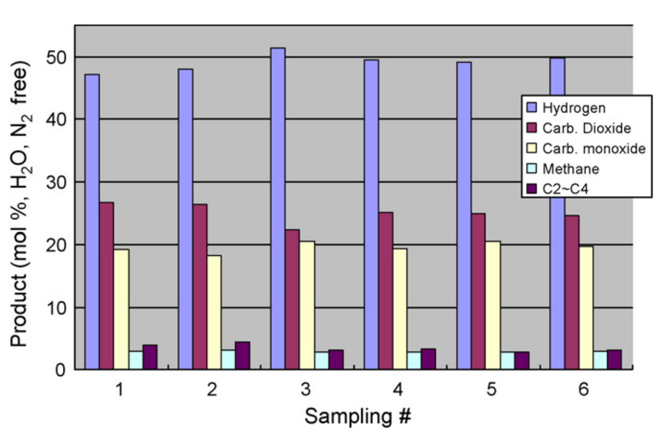

Fig. 3. Product distributions obtained from non-UI reformer (synthetic diesel, $H_2O/C = 1.25$, $O_2/C = 0.5$, 5000 h^{-1}, CGO-Pt, furnace temperature = 800 °C, average fuel conversion = 82.3%).

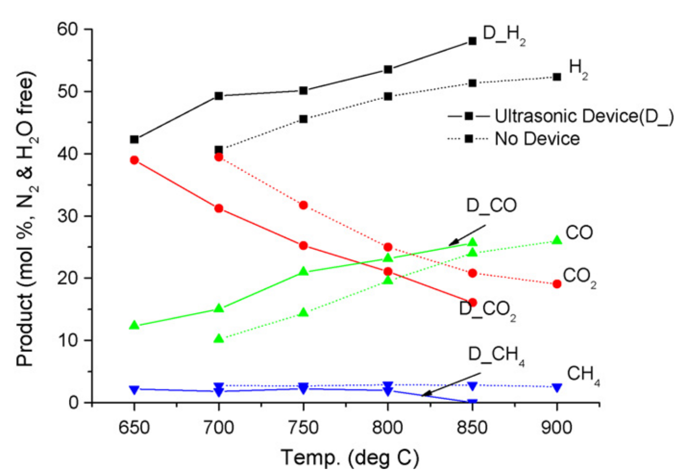

Fig. 5. Product distributions after reforming according to UI usage (synthetic diesel, $O_2/C = 0.5$, $H_2O/C = 1.25$, GHSV = 5000 h^{-1}).

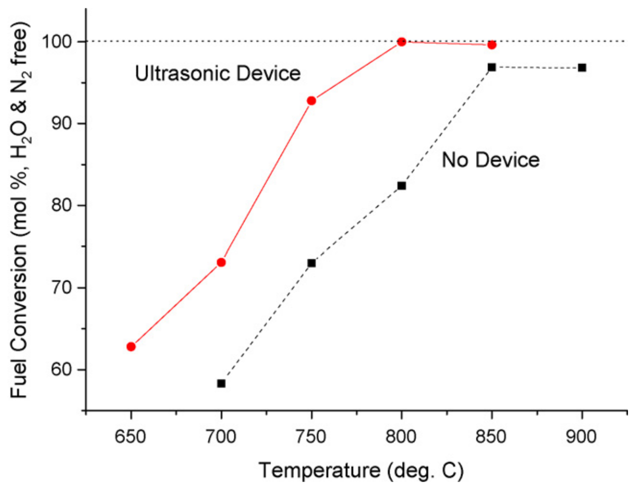

Fig. 6. Fuel conversion of UI and non-UI reformer according to furnace temperature.

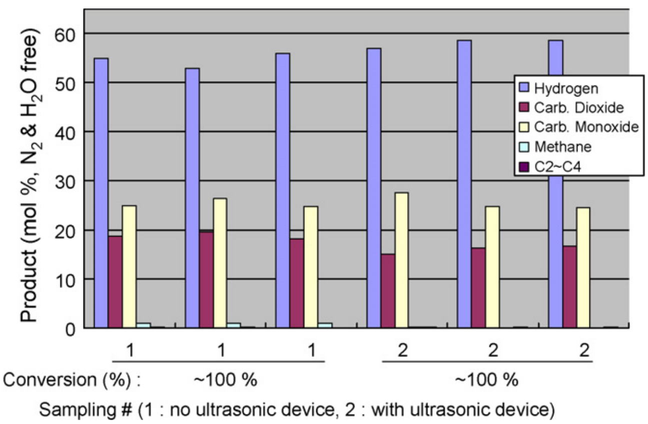

Fig. 8. Product distributions obtained from synthetic diesel reforming according to UI usage (synthetic diesel, $H_2O/C = 1.25$, $O_2/C = 0.5$, GHSV = 5000 h^{-1}, CGO-Pt, 850 °C).

hand, the RE of synthetic diesel using the UI is 87%. It is greater than the RE of $C_{16}H_{34}$ non-UI reforming and the RE of synthetic diesel non-UI reforming.

For the UI and the non-UI reformer, we have compared reformate gas compositions (Fig. 8) and upper temperatures of the catalyst bed (Fig. 9) to demonstrate the effect of the UI on reforming performance. Hydrocarbons are almost negligible in the UI reformer, as indicated in Fig. 8.

The upper temperatures of the catalyst bed in each case are given in Fig. 9. Lower temperatures, as much as 20 °C less, are obtained when the UI is used to reform the synthetic diesel compared with the non-UI reformer. Comparing the temperature difference and reforming efficiencies, it can be deduced why the ultrasonic device enhances the reforming efficiency. One reason is the reduced energy needed for diesel vapourization. The atomization of diesel can lower the amount of latent heat by widening the actual open surface where the heat transfer occurs [14]. This promotes the evaporation of diesel and the formation of a mixture with the oxidants. The temperature at the front of the catalyst bed decreases with the effective vapourization of diesel. As a result, well-mixed reactants enhance the reforming efficiency. Another reason is the inhibition of undesired non-catalytic reactions at the front of the catalyst bed of the UI-reformer. As previously reported [15], the reforming process progresses not only on the catalyst surface but also in a non-catalytic zone, due to high reforming temperatures (about 850 °C). At these high temperatures, most of the paraffinic heavier hydrocarbons are converted into light hydrocarbons with a variety of hydrocarbon structures by oxidation and thermal pyrolysis, before reaching the catalyst surface. Inhomogeneous mixing can lead to unwanted fuel consumption due to unstable combustion in a specific fuel-rich area. This will cause a decrease in the reforming efficiency. In addition, olefinic and aromatic compounds, which have low reforming reaction rates, usually form during the decomposition of heavier hydrocarbons. The reforming efficiency decreases because of the undesirable delivery process of the fuel. The UI allows for the formation of a homogeneous mixture, which inhibits the fuel consumption and its transformation into undesired species. Therefore, it is believed that the reforming efficiency and fuel conversion are both greatly influenced by the fuel delivery methods.

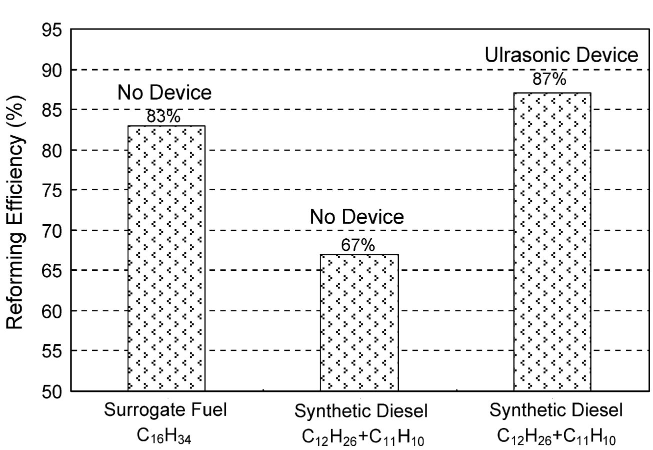

Fig. 7. Reforming efficiency (%) ($H_2O/C = 1.25$, $O_2/C = 0.5$, GHSV = 5000 h^{-1}, 850 °C, RE = (LHV of H_2 and CO/LHV of fuel)).

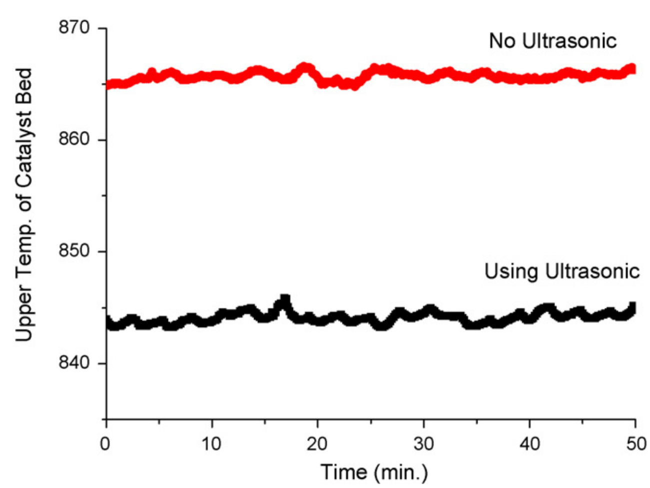

Fig. 9. Upper temperature vs. time with and without UI ($H_2O/C = 1.25$, $O_2/C = 0.5$, GHSV = 5000 h^{-1}, 850 °C).

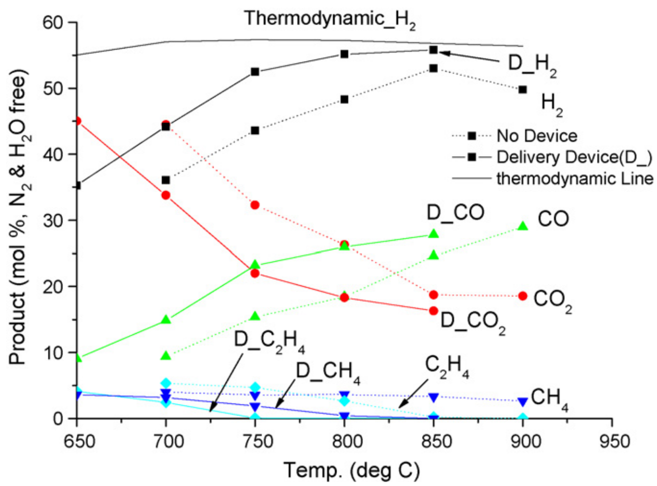

Fig. 10. Product distribution using commercial diesel reforming ($C_{16}H_{34}$ thermodynamic data, $H_2O/C = 1.25$, $O_2/C = 0.5$ on the basis of synthetic diesel, CGO-Pt).

After the operating conditions were determined by using synthetic diesel, commercial diesel reforming was performed. The amount of H_2 obtained in the UI reformer is much greater than that in the non-UI reformer, as shown in Fig. 10. The H_2 yield is even close to the thermodynamic equilibrium state (TES) with respect to $C_{16}H_{34}$.

On the basis of these results, a 100-W_e-class, self-sustaining, diesel reformer was developed, as shown schematically in Fig. 11. The UI is located at the top of the reactor to deliver the diesel. A water line for vapourization is in contact with the reactor wall like a coiled spring. Air is injected through an ultrasonic device (separate from the fuel line). The air is not only an oxidant but also acts as a shield, which can prevent atomized diesel from attaching to the reactor wall. In addition, it cools down the piezoelectric transducer. The inside of the reactor consists of a mixing bed using zirconia balls (diameter: 3.08 mm) and a catalytic bed using CGO-Pt, as depicted in Fig. 11. An electrical heating coil powered by a small battery (12 V, 9 Ah) was installed between the catalyst bed and mixing bed, for start-up of the reformer. Ceramic wool was used to insulate the reactor. Fourteen thermocouples were used to monitor the reforming reaction (8 inner, 6 outer). The design of the self-sustaining diesel UI reformer is shown in Fig. 12.

In the start-up process of the reformer, low power consumption and minimal time are required. The start-up conditions inevitably pass through the thermodynamic coke formation zone [15]. Therefore, rapid start-up should be attained to avoid severe carbon deposition. Diesel autothermal reforming is started by lighting off the fuel and air mixture. The mixing ratio is a dominant factor which governs both the start-up time and the amount of carbon deposition during the oxidation reaction [9]. Once the reaction temperature is reached, it is controlled by the mixing ratio and flowrates of the reactants fuel, air, and water. It requires, however, a delicate control strategy due to the high possibility of severe carbon deposition, even in the thermodynamic carbon-free zone. The process of decreasing the reaction temperature (e.g., low O_2/C) must be much more elaborate than the process of increasing the reaction temperature (e.g., high O_2/C). In addition, the control of the mixing ratio directly affects the reforming efficiency by changing the amount of H_2 in the reformate gas [15,19]. This feature is not discussed here.

In the present reactor, H_2O/C, O_2/C, and GHSV are 1.25, 0.56 and 12,500 h^{-1}, respectively. Start-up of the reformer is initiated by an electrical heating coil which supplies heat energy until the light-off temperature (~250 °C) of the fuel and air mixture is reached. The temperature then increases to about 400 °C (Fig. 13). Several seconds later, all the reactants are supplied for ATR operation. Finally, steady-state ATR operation can be

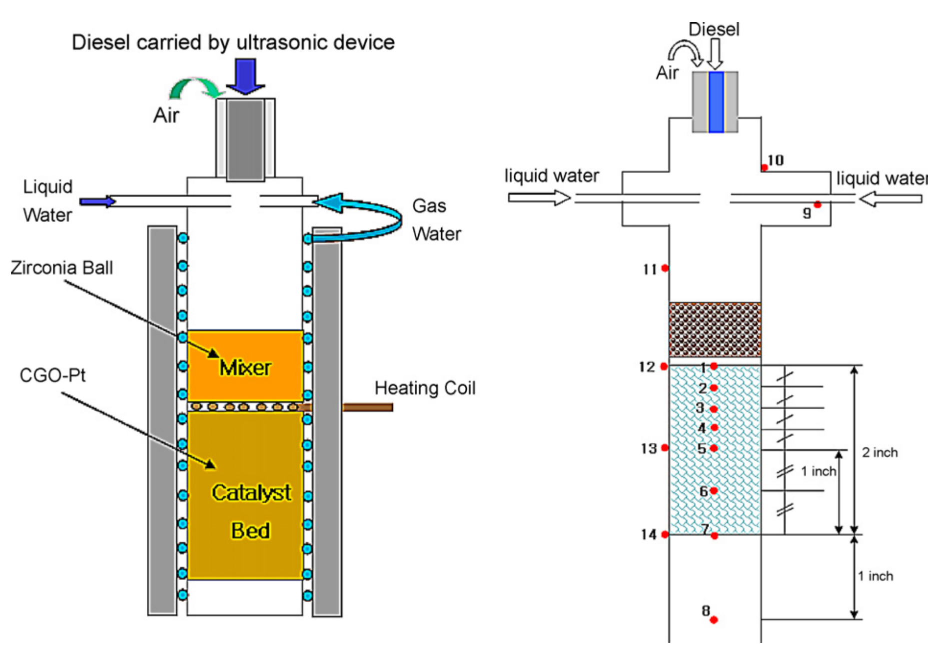

Fig. 11. Schematic diagram and positions of thermocouples.

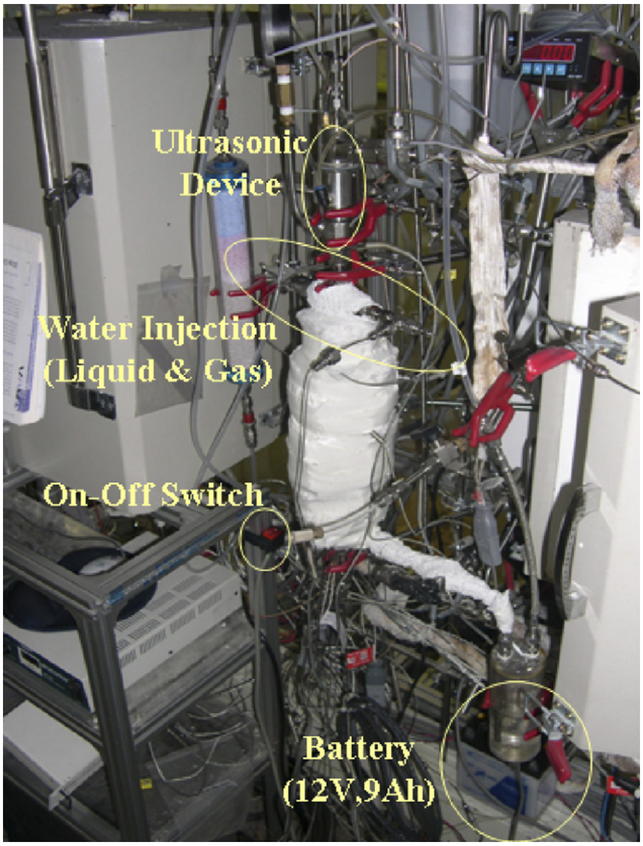

Fig. 12. Actual experimental set-up.

achieved, as described in Fig. 14. External energy consumption for start-up of the reformer is about 100-W_e for about 10 min. If more power is supplied to the heating coil, the start-up time will decrease.

The temperatures at each position (described in Fig. 11) for 21 h are shown in Fig. 14. Although transient behaviour is seen initially, most of the temperatures are steady, except for a slight decrease in the temperatures of T/C 1 and T/C 2, which are located at the front of the catalyst bed.

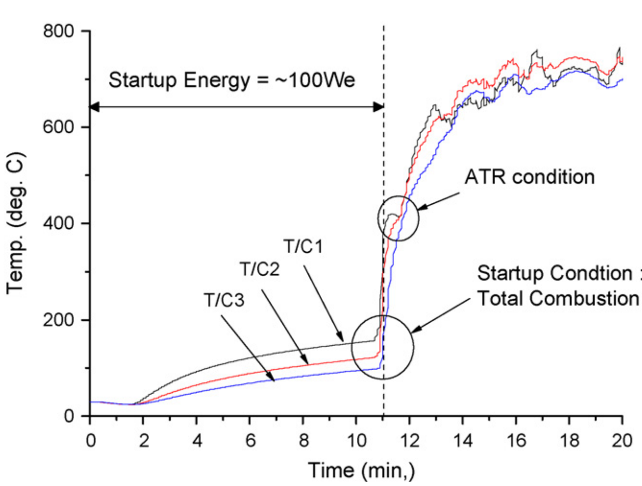

Fig. 13. Catalyst temperature during start-up (start-up conditions: synthetic diesel = 0.2 ml min^{-1} (l), air = 1990 ml min^{-1} (g)).

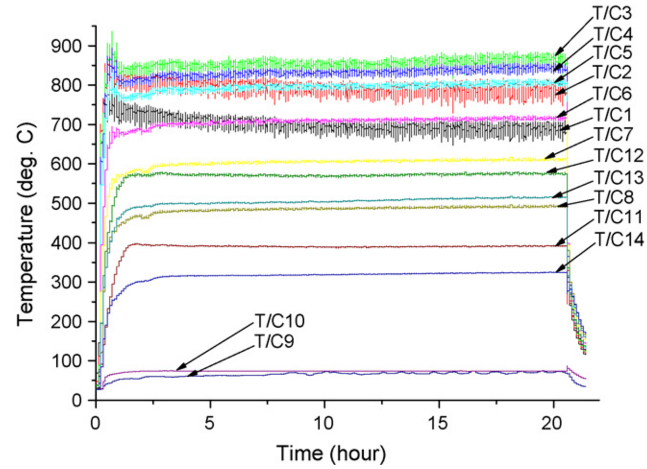

Fig. 14. Temperatures at each point for 24 h operation (synthetic diesel, $H_2O/C = 1.25$, $O_2/C = 0.56$, GHSV = ~12,500 h^{-1}, CGO-Pt).

The average inner and wall temperatures along the reactor are given in Fig. 15. As the length of the catalyst bed increases, the inner temperature also increases until $x = 0.5$ in. and then the temperature continuously decreases with increased catalyst bed length. It is well-known that the heat energy from the initial oxidation leads to sequential endothermic steam reforming, which results in the temperature profile shown in Fig. 15 [15]. The fuel conversion and reformate gas composition for 21 h are given in Fig. 16. Average fuel conversion is 85%. The H_2 yield decreases slightly with increasing operation time because of carbon deposition. As seen in Fig. 17, the amount of C_2H_4 increases, which indicates an increase in carbon deposition because it is representative of a carbon precursor [4].

Using the self-sustaining reactor, commercial diesel reforming was performed. The product compositions with increasing operation time are given in Fig. 18. The results are very similar to those obtained from synthetic diesel reforming (Fig. 17). After 26 h of operation, the reforming performance, especially the relative amount of H_2, decreases suddenly due to severe carbon deposition. As presented in Fig. 18, the initial reform-

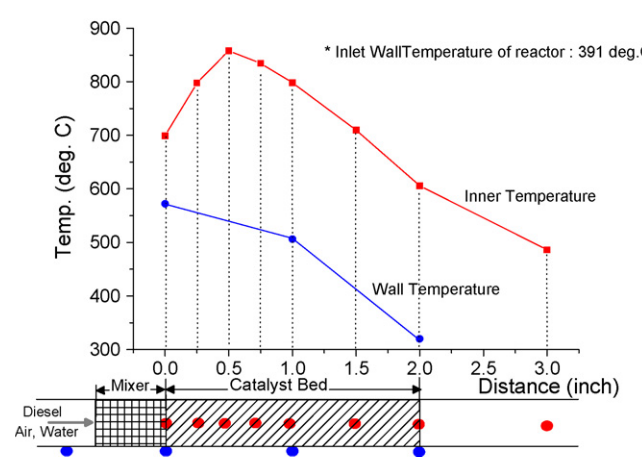

Fig. 15. Average temperatures at each point (lower figure describes T/C positions) (synthetic diesel, $H_2O/C = 1.25$, $O_2/C = 0.56$, GHSV = ~12,500 h^{-1}, CGO-Pt).

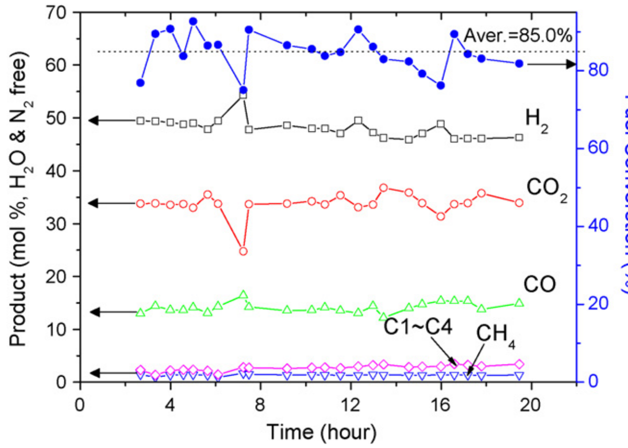

Fig. 16. Product distribution vs. time (synthetic diesel, $H_2O/C = 1.25$, $O_2/C = 0.56$, $GHSV = \sim 12{,}500\ h^{-1}$, CGO-Pt).

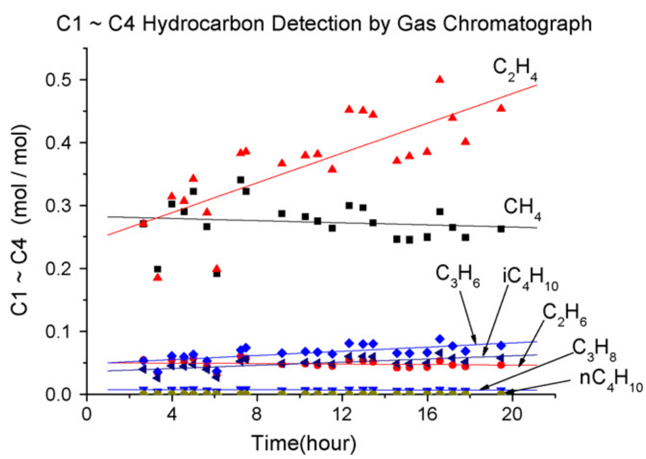

Fig. 17. Hydrocarbons in reformate gas vs. time (synthetic diesel, $H_2O/C = 1.25$, $O_2/C = 0.56$, $GHSV = \sim 12{,}500\ h^{-1}$, CGO-Pt).

ing temperatures at all positions increase with the progression of carbon deposition. The increase in temperature can be explained by the decrease in steam reforming, which has a relatively low reaction rate compared with the oxidation reaction with decreasing active surface of the catalyst. All the temperatures increase continuously until 113 min (see Fig. 19) and then the temperatures (1, 2, 3 and 4) at the front half of catalyst bed decrease rapidly. On the other hand, the temperatures (5, 6 and 7) at the rear half of the catalyst bed increase. The deactivation of the catalyst by carbon deposition during autothermal reforming, is indicated by the data in Fig. 20. If zero minutes is defined as the starting point of rapid degradation of performance due to carbon deposition, it takes about 15 min to deactivate the reforming. The initial temperature profiles at 0, 4, and 9 min increase with the progression of carbon deposition. As solid carbon deposits on the catalyst surface, the chemical function of the catalyst decreases sharply from the front to the rear of the catalyst bed. This causes the rear temperatures of the catalyst bed at 9 and 13 min to increase. Finally, all temperatures decrease due to deactivation of the catalyst.

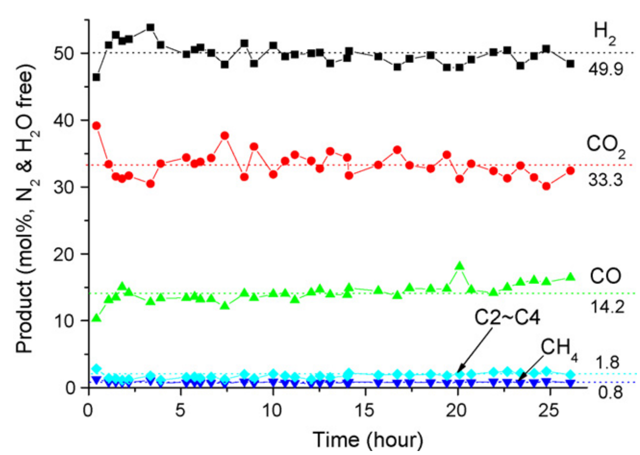

Fig. 18. Product distribution obtained by commercial diesel reforming vs. time (diesel, CGO-Pt, $H_2O/1.25$, $O_2/C = 0.5$, $GHSV = 12{,}500\ h^{-1}$ calculated on a synthetic diesel base).

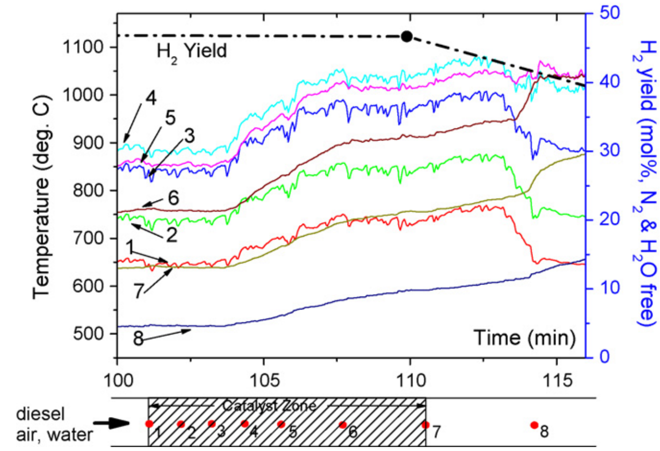

Fig. 19. Temperature of catalyst bed at sudden degradation.

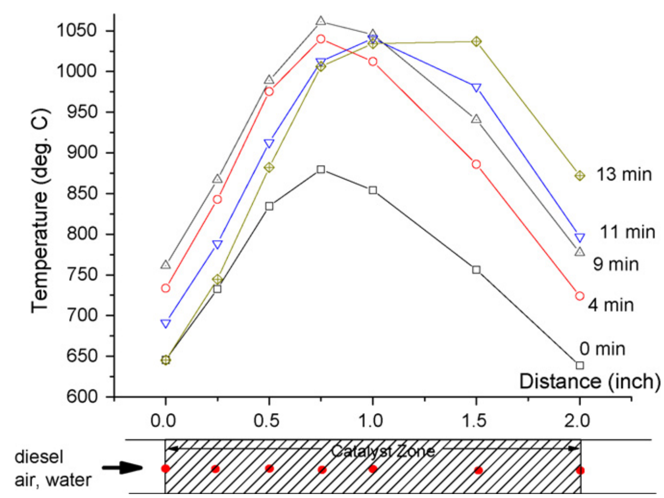

Fig. 20. Temperature vs. length of catalyst according to operation time.

4. Conclusions

An effective fuel-delivery system for heavier hydrocarbons such as kerosene, diesel and JP-8 is required. Fuel delivery is not merely an engineering issue, but is a fundamental issue that affects the reforming chemistry on the catalyst surface. Therefore, the method of fuel delivery is deeply associated with the reforming efficiency. An ultrasonic injector is one option to supply the fuels for the reforming system. The reforming efficiency increased by about 20% in the micro-reactor when the UI was used. This improvement may be caused by inhibition of the reactions that occur at high temperatures in the non-catalytic mixing zone that is located before the catalyst bed. Poorly mixed fuel and oxidant lead to gas phase reactions, such as combustion at high fuel/air ratios in the non-catalytic mixing zone. During oxygen rich or lean combustion (or partial oxidation), the aromatic and olefin components may cause the reforming kinetics to slow down. It is very difficult to explain the effects of the UI on the reforming efficiency. More detailed experiments, investigating the effects of the mixture on the reforming chemistry, will be performed. By using the UI, a 100-W_e self-sustaining reactor has been designed for diesel autothermal reforming. Start-up and steady-state operation of the reactor is performed. It is found that carbon deposition progresses very quickly in the reformer and deactivates the reforming catalyst after 15 min.

Acknowledgments

This work was funded by the Korea Institute of Machinery and Materials (KIMM). Analysis facilities, such as the GC–MS and the SEM/EDX, were supported by the Ministry of Education and Human Resources Development.

References

[1] J.P. Kopasz, D. Applegate, L. Miller, H.K. Liao, S. Ahmed, Int. J. Hydrogen Energy 30 (2005) 1243–1250.
[2] P.K. Cheekatamarla, W.J. Thomson, Appl. Catal. A: Gen. 287 (2005) 176–182.
[3] A. Shamsi, J.P. Baltrus, J.J. Spivey, Appl. Catal. 293 (2005) 145–152.
[4] F. Joensen, J.R. Rostrup-Nielsen, J. Power Sources 105 (2002) 195–201.
[5] D.-J. Liu, T.D. Kan, H.-K. Liao, S. Ahmed, Int. J. Hydrogen Energy 29 (2004) 1035–1046.
[6] M. Flytzani-Stephanopoulos, G.E. Voecks, Int. J. Hydrogen Energy 7 (1983) 539–548.
[7] R.L. Borup, M.A. Inbody, T.A. Semelsberger, J.I. Tafoya, D.R. Guidry, Catal. Today 99 (2005) 263–270.
[8] T.R. Krause, S. Ahmed, R. Kumar, The 4th International Conference on Fuel Cell Science, Engineering and Technology, Proceedings of Fuel Cell 2006, FUELCELL2006-97260.
[9] I. Kang, J. Bae, J. Hong, S. Lim, S. Lee, G. Bae, KSME 2006 Spring Annual Meeting, KSME06S Th14F014.
[10] X. Ma, L. Sun, C. Song, Catal. Today 77 (2005) 107–116.
[11] B. Lenz, T. Aicher, J. Power Sources 149 (2005) 44–52.
[12] C. Palm, P. Cremer, R. Peters, D. Stolten, J. Power Sources 106 (2002) 231–237.
[13] M. Krumpelt, T.R. Krause, J.D. Carter, J.P. Kopasz, S. Ahmed, Catal. Today 77 (2002) 3–16.
[14] L. Hartmann, K. Lucka, H. Köhne, J. Power Sources 118 (2003) 286–297.
[15] I. Kang, J. Bae, J. Power Sources 159 (2006) 1283–1290.
[16] I. Kang, J. Bae, G. Bae, J. Power Sources 163 (2006) 538–546.
[17] I. Kang, J. Bae, H. Jee, Y. Song, 2006 Spring Conference Proceeding of KSAE, vol. 2, 2006, pp. 1884–1890.
[18] I. Kang, J. Bae, H. Jee, G. Bae, Y. Yoo, Proceedings of the KSME 2005 Spring Annual Meeting, KSME 05S344.
[19] S. Ahmed, M. Krumpelt, Int. J. Hydrogen Energy 26 (2001) 191–301.